Towards NLO-BFKL From Glauber-SCET

SCET 2024, Salamanca

Aditya Pathak

With Anjie Gao and Gherardo Vita

April 15, 2024

Outline

Outline

The high energy limit

Rapidity evolution via BFKL equation

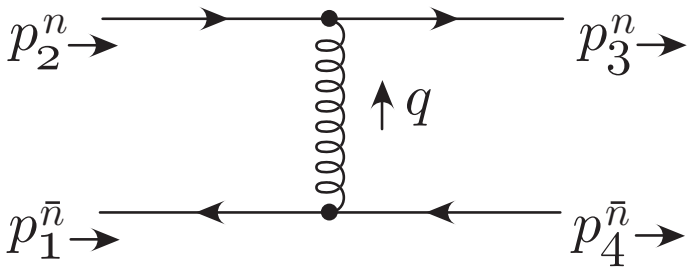

- Three fundamental limits:

  soft, collinear and Regge.
- Forward scattering regime involves large logarithms of $x \sim \frac{t}{s}$
- The BFKL equation describes this rapidity evolution in the x.

See Anjie Gao's talk.

Two lines of attack to describe Regge behavior in cross-sections:

- Unitarization of cross-section leading to nonlinear generalizations of BFKL.
- Achieve consistent collinear and BFKL resummation: ← This talk

The high energy limit

Rapidity evolution via BFKL equation

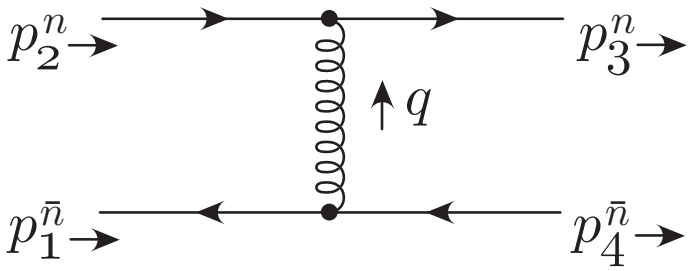

- Three fundamental limits:

  soft, collinear and Regge.
- Forward scattering regime involves large logarithms of $x \sim \frac{t}{s}$
- The BFKL equation describes this rapidity evolution in the x.

See Anjie Gao's talk.

Two lines of attack to describe Regge behavior in cross-sections:

- Unitarization of cross-section leading to nonlinear generalizations of BFKL.
- Achieve consistent collinear and BFKL resummation: ← This talk

Spoiler alert!

- NLO-BFKL Kernel known since 1998 (Fadin & Lipatov). [FL98]

Importance of higher order small-x_b resummation

Small-x data at N^{3}LO plays a crucial role in improving PDFs

- N^{3}LO pieces available from BFKL evolution of the splitting functions [McG+23]:

P_{gg}: $\alpha_s^3 \ln^3 x$ ✓, $\alpha_s^3 \ln^2 x$ ✓, $\alpha_s^3 \ln x$ (?)

P_{gq}: $\alpha_s^3 \ln^3 x$ ✓, $\alpha_s^3 \ln^2 x$ (?)

P_{qg}: $\alpha_s^3 \ln^2 x$ ✓, $\alpha_s^3 \ln x$ (?)

$P_{qq}^{\rm PS}$: $\alpha_s^3 \ln^2 x$ ✓, $\alpha_s^3 \ln x$ (?)

- Compare P_{gg} and P_{gq}: Difference in moments (MSHT, 4 vs. NNPDF, 5) only impacts large x region.
- P_{gq} has the highest power of missing logarithm $\rightarrow$ large uncertainty in the small-x region.

Comparison with MSHT and NNPDF versions

Slide from Robert Thorne, DIS 2024

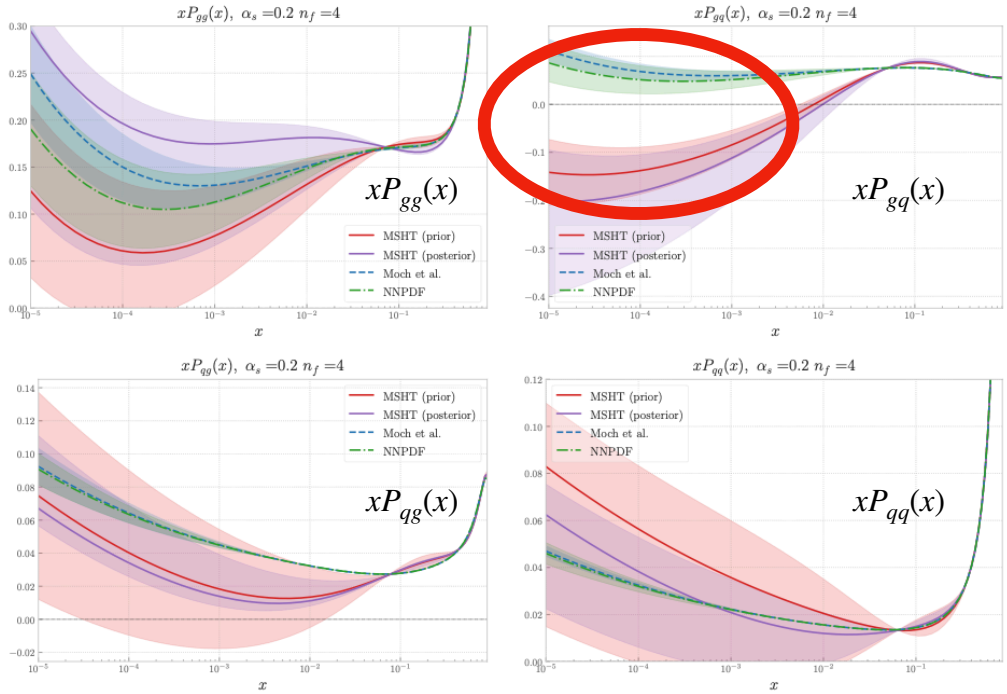

Importance of higher order small-x_b resummation

Small-x data at N^{3}LO plays a crucial role in improving PDFs

- N^{3}LO pieces available from BFKL evolution of the splitting functions [McG+23]:

P_{gg}: $\alpha_s^3 \ln^3 x$ ✓, $\alpha_s^3 \ln^2 x$ ✓, $\alpha_s^3 \ln x$ (?)

P_{gq}: $\alpha_s^3 \ln^3 x$ ✓, $\alpha_s^3 \ln^2 x$ (?)

P_{qg}: $\alpha_s^3 \ln^2 x$ ✓, $\alpha_s^3 \ln x$ (?)

$P_{qq}^{\rm PS}$: $\alpha_s^3 \ln^2 x$ ✓, $\alpha_s^3 \ln x$ (?)

- Compare P_{gg} and P_{gq}: Difference in moments (MSHT, 4 vs. NNPDF, 5) only impacts large x region.
- P_{gq} has the highest power of missing logarithm $\rightarrow$ large uncertainty in the small-x region.

Comparison with MSHT and NNPDF versions

Slide from Robert Thorne, DIS 2024

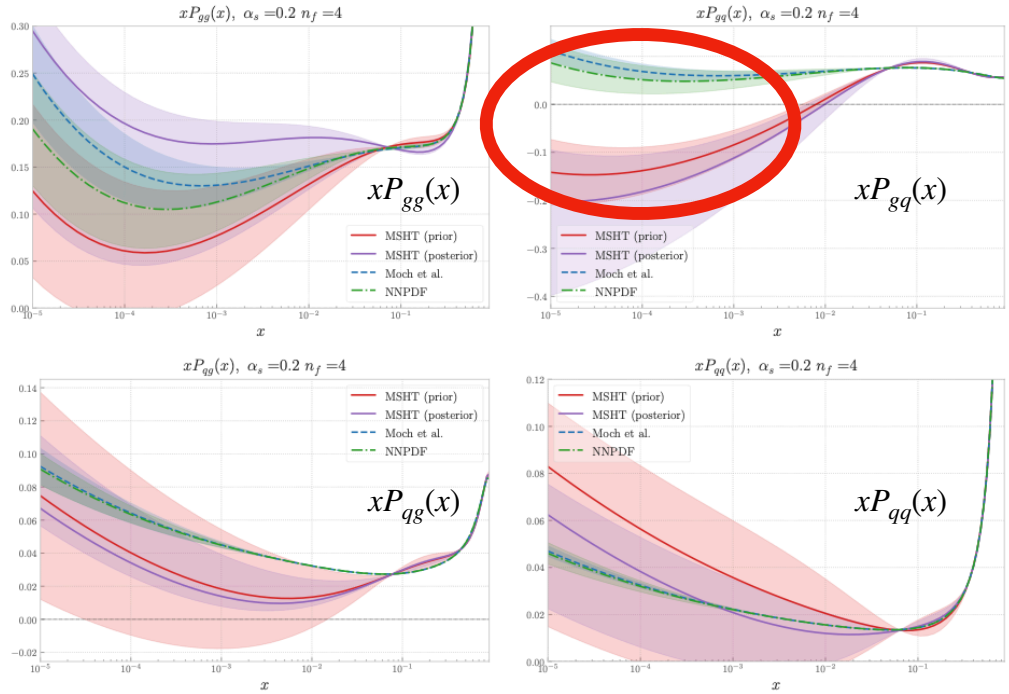

Why has been achieving NLL$_x$ P_{ij} so challenging?

The tangled nature of BFKL and Twist factorization

Inclusive DIS Review

- Focus on inclusive cross sections. Take DIS as an example:
- Twist factorization in DIS:

$$\frac{1}{x_b} F_a(x_b, Q^2) = \sum_\kappa \int_{x_b}^1 \frac{\mathrm{d}\xi}{\xi} H_a^{(\kappa)}\left(\frac{x_b}{\xi}, Q, \mu\right) f_{\kappa/p}(\xi, \mu) + \mathcal{O}\left(\frac{\Lambda^2_{\mathrm{QCD}}}{Q^2}\right).$$

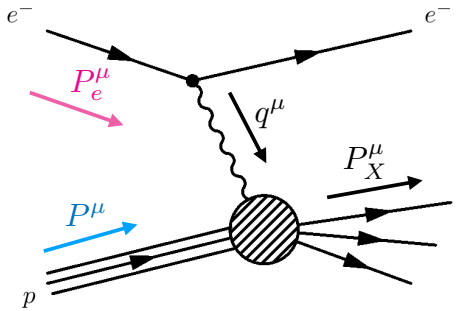

Mellin transform: $\quad \bar{f}(n) \equiv \int_0^1 \frac{dx}{x} x^{n+1} f(x)$

$$\bar{F}_a^{(\kappa)}(N) = \sum_{\kappa'} \bar{H}_a^{(\kappa')}(N) \times \underbrace{\bar{\Gamma}_{\kappa'\kappa}\left(N, \epsilon\right)}_{\text{PDF}} \qquad \bar{\Gamma}_{\kappa'\kappa}\left(\alpha_s(\mu^2), N, \epsilon\right) \equiv \mathrm{P}\ \exp\left(\int_0^{\alpha_s(\mu^2)} \frac{d\alpha}{\beta(\epsilon, \alpha)} \gamma^s(\alpha, N)\right)_{\kappa'\kappa}$$

The tangled nature of BFKL and Twist factorization

Inclusive DIS Review

- Focus on inclusive cross sections. Take DIS as an example:
- Twist factorization in DIS:

$$\frac{1}{x_b} F_a(x_b, Q^2) = \sum_\kappa \int_{x_b}^1 \frac{\mathrm{d}\xi}{\xi} H_a^{(\kappa)}\left(\frac{x_b}{\xi}, Q, \mu\right) f_{\kappa/p}(\xi, \mu) + \mathcal{O}\left(\frac{\Lambda^2_{\mathrm{QCD}}}{Q^2}\right).$$

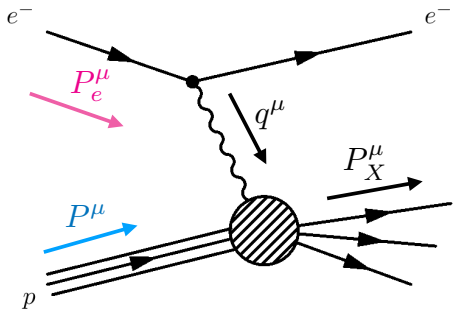

Mellin transform: $\bar{f}(n) \equiv \int_0^1 \frac{dx}{x} x^{n+1} f(x)$

$$\bar{F}_a^{(\kappa)}(N) = \sum_{\kappa'} \bar{H}_a^{(\kappa')}(N) \times \underbrace{\bar{\Gamma}_{\kappa'\kappa}\left(N, \epsilon\right)}_{\text{PDF}} \qquad \bar{\Gamma}_{\kappa'\kappa}\left(\alpha_s(\mu^2), N, \epsilon\right) \equiv \mathrm{P}\ \exp\left(\int_0^{\alpha_s(\mu^2)} \frac{d\alpha}{\beta(\epsilon, \alpha)} \gamma^s(\alpha, N)\right)_{\kappa'\kappa}$$

- Terms retained at leading twist:
- Includes both perturbative ($\bar{H}_a^{(\kappa)}(N)$) and nonperturbative ($\gamma^s(\alpha_s, N)$) pieces

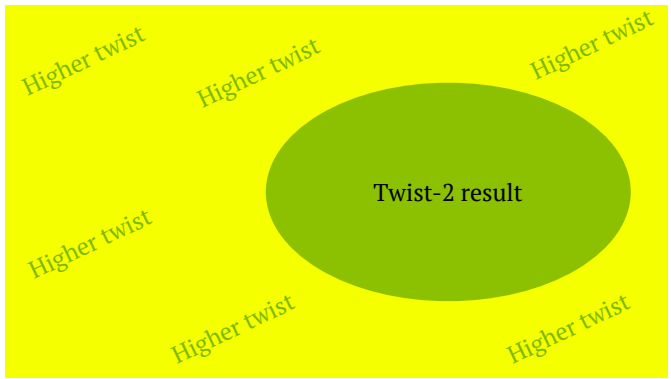

The tangled nature of BFKL and Twist factorization

Inclusive DIS Review

- Focus on inclusive cross sections. Take DIS as an example:
- Twist factorization in DIS:

$$\frac{1}{x_b} F_a(x_b, Q^2) = \sum_\kappa \int_{x_b}^1 \frac{\mathrm{d}\xi}{\xi} H_a^{(\kappa)}\left(\frac{x_b}{\xi}, Q, \mu\right) f_{\kappa/p}(\xi, \mu) + \mathcal{O}\left(\frac{\Lambda^2_{\mathrm{QCD}}}{Q^2}\right).$$

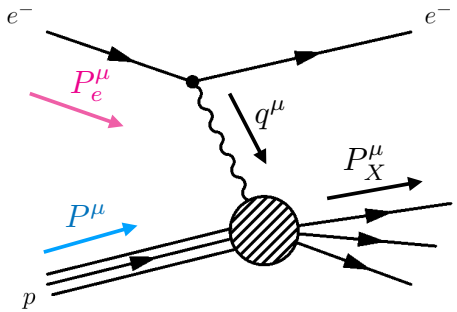

Mellin transform: $\quad \bar{f}(n) \equiv \int_0^1 \frac{dx}{x} x^{n+1} f(x)$

$$\bar{F}_a^{(\kappa)}(N) = \sum_{\kappa'} \bar{H}_a^{(\kappa')}(N) \times \underbrace{\bar{\Gamma}_{\kappa'\kappa}\left(N, \epsilon\right)}_{\text{PDF}} \qquad \bar{\Gamma}_{\kappa'\kappa}\left(\alpha_s(\mu^2), N, \epsilon\right) \equiv \mathrm{P}\ \exp\left(\int_0^{\alpha_s(\mu^2)} \frac{d\alpha}{\beta(\epsilon, \alpha)} \gamma^s(\alpha, N)\right)_{\kappa'\kappa}$$

- Consider an expansion with $\lambda \sim x_b$ as the power counting parameter
- This isolates the leading pieces in the structure function F_a that scale as $\sim 1/x_b$

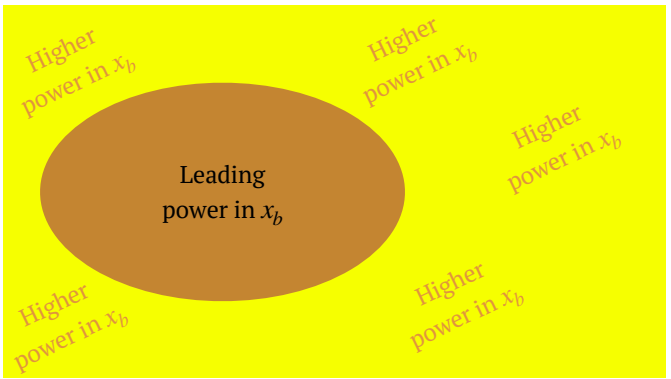

The tangled nature of BFKL and Twist factorization

Nontrivial overlap between twist and small-x_b expansions

- Leading terms in $x_b \to 0$ limit:

$$\frac{1}{x}\ln^{\ell-1}(x) \quad \to \quad \frac{1}{n^\ell}$$

- Small-x_b limit includes leading as well as higher-twist pieces.

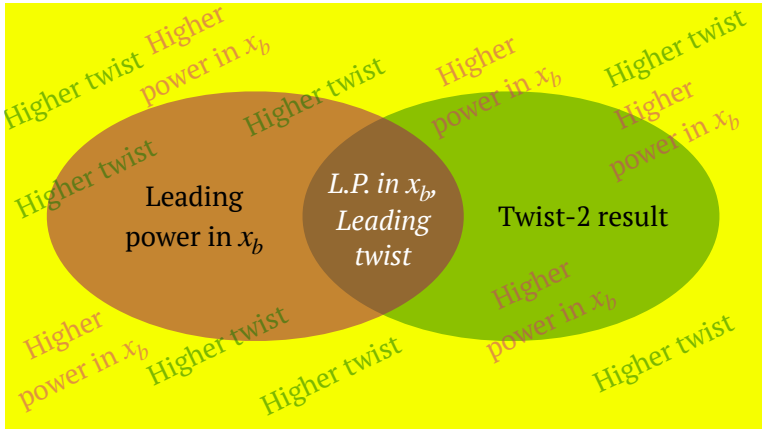

$$\bar{H}_L^{(g)}(n) \quad \sim \quad \alpha_s \quad + \quad \alpha_s\frac{\alpha_s}{n} \quad + \quad \alpha_s\left(\frac{\alpha_s}{n}\right)^2 \quad + \quad \alpha_s\left(\frac{\alpha_s}{n}\right)^3 \quad + \ldots ,$$

The tangled nature of BFKL and Twist factorization

Nontrivial overlap also of IR poles between twist and small-x_b expansions

- Leading terms in $x_b \to 0$ limit:

$$\frac{1}{x}\ln^{\ell-1}(x) \quad \to \quad \frac{1}{n^\ell}$$

$$\bar{\Gamma}_{\kappa'\kappa}\left(\alpha_s(\mu^2), N, \epsilon\right) \equiv \mathrm{P}\ \exp\left(\int_0^{\alpha_s(\mu^2)} \frac{d\alpha}{\beta(\epsilon,\alpha)}\gamma^s(\alpha, N)\right)_{\kappa'\kappa}$$

- Small-x_b limit includes leading as well as higher-twist pieces.
- Nontrivial overlap also of IR poles

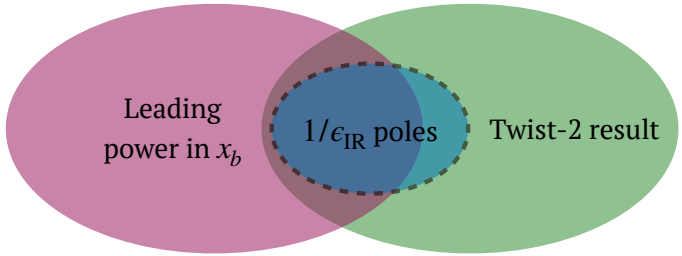

$$\begin{aligned}
\bar{H}_L^{(g)}(n) &\sim \alpha_s + \alpha_s\frac{\alpha_s}{n} + \alpha_s\left(\frac{\alpha_s}{n}\right)^2 + \alpha_s\left(\frac{\alpha_s}{n}\right)^3 + \dots, \\
\gamma_{gg}(n) &\sim \frac{\alpha_s}{n} + \left(\frac{\alpha_s}{n}\right)^2 + \left(\frac{\alpha_s}{n}\right)^3 + \left(\frac{\alpha_s}{n}\right)^4 + \dots, \\
\gamma_{qg}(n) &\sim \alpha_s + \alpha_s\frac{\alpha_s}{n} + \alpha_s\left(\frac{\alpha_s}{n}\right)^2 + \alpha_s\left(\frac{\alpha_s}{n}\right)^3 + \dots.
\end{aligned}$$

- Collinear poles $\frac{\alpha_s}{\epsilon}$ have a different origin than BFKL-generated IR poles $\frac{1}{\epsilon}\frac{\alpha_s}{n}$.

Outline

Kinematics associated with the small-x_b region

A recap of small-x factorization presented last year [NPS23]

- Center of mass light cone coordinates:

$$P^\mu = \frac{\sqrt{s}}{2} n^\mu \,, \qquad P_e^\mu = \frac{\sqrt{s}}{2} \bar{n}_\mu$$

- Power counting parameters:

$$\lambda' \sim \frac{\Lambda_{\rm QCD}}{Q} \quad \text{and} \quad \lambda \sim x_b \,.$$

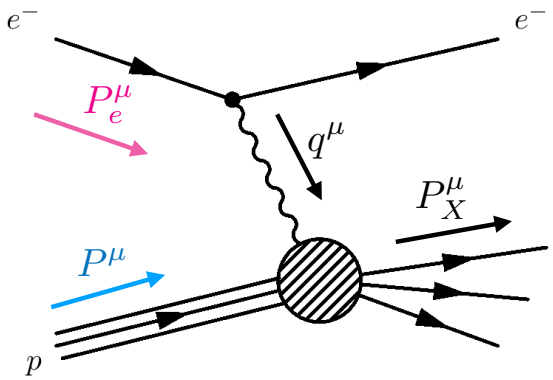

	Hard scattering		**Forward scattering**
$\dfrac{P_X^2}{s} = \dfrac{(q+P)^2}{s} = \dfrac{Q^2}{s}\dfrac{(1-x_b)}{x_b}$	$\sim \lambda^0$	or	$\sim \lambda$
$q^\mu = -\dfrac{Q^2}{\sqrt{s}}\dfrac{n^\mu}{2} + \dfrac{Q^2}{x_b\sqrt{s}}\dfrac{\bar{n}^\mu}{2} + q_\perp^\mu$	$\sim \sqrt{s}\left(1, \lambda, \sqrt{\lambda}\right)$	or	$\sim \sqrt{s}\left(\lambda, \lambda^2, \lambda\right)$

Kinematics associated with the small-x_b region

A recap of small-x factorization presented last year [NPS23]

- Center of mass light cone coordinates:

$$P^\mu = \frac{\sqrt{s}}{2} n^\mu , \qquad P_e^\mu = \frac{\sqrt{s}}{2} \bar{n}_\mu$$

- Power counting parameters:

$$\lambda' \sim \frac{\Lambda_{\rm QCD}}{Q} \quad \text{and} \quad \lambda \sim x_b \ .$$

$$p_{\bar{n}} \sim \sqrt{s}\big(\underbrace{1}_{p^+}, \underbrace{\lambda^2}_{p^-}, \underbrace{\lambda}_{p_\perp}\big)$$

q_γ

$$k_s \sim \sqrt{s}\big(\underbrace{\lambda}_{p^+}, \underbrace{\lambda}_{p^-}, \underbrace{\lambda}_{p_\perp}\big)$$

q_G

$$p_n \sim \sqrt{s}\big(\underbrace{\lambda^2}_{p^+}, \underbrace{1}_{p^-}, \underbrace{\lambda}_{p_\perp}\big)$$

	Hard scattering		**Forward scattering**
$\dfrac{P_X^2}{s} = \dfrac{(q+P)^2}{s} = \dfrac{Q^2}{s}\dfrac{(1-x_b)}{x_b}$	$\sim \lambda^0$	or	$\sim \lambda$
$q^\mu = -\dfrac{Q^2}{\sqrt{s}}\dfrac{n^\mu}{2} + \dfrac{Q^2}{x_b\sqrt{s}}\dfrac{\bar{n}^\mu}{2} + q_\perp^\mu$	$\sim \sqrt{s}\big(1, \lambda, \sqrt{\lambda}\big)$	or	$\sim \sqrt{s}\big(\lambda, \lambda^2, \lambda\big)$

Need a soft sector : $k_s^\mu \sim \sqrt{s}\big(\lambda, \lambda, \lambda\big)$ and Glauber modes : $q_G^\mu \sim \sqrt{s}\big(\lambda^2, \lambda, \lambda\big)$

Small-x factorization in Glauber-SCET

A recap of small-x factorization presented last year [NPS23]

Collinear-soft interactions are mediated via the *ns*-Glauber action (Rothstein, Stewart '16) [RS16]:

$$S_G^{ns} = 8\pi\alpha_s \sum_{i,j,A} \int \mathrm{d}^d y \int \mathrm{d}^d x \int \frac{\mathrm{d}^d q'}{(2\pi)^d} \frac{e^{\mathrm{i}(x-y)\cdot q'}}{q_\perp'^2} \mathcal{O}_n^{iA}(x)\mathcal{O}_s^{j_n A}(y)\,,$$

$$\mathcal{O}_{n_i}^{qA} = \bar{\chi}_{n_i} \mathbf{T}_i^A \frac{\bar{\not{n}}_i}{2} \chi_{n_i}\,, \qquad \mathcal{O}_{n_i}^{gA} = \frac{1}{2}\mathcal{B}_{n\perp\mu}^B (\mathrm{i}f^{ABC}) \frac{\bar{n}_i}{2} \cdot (\mathcal{P} + \mathcal{P}^\dagger)\mathcal{B}_{n\perp}^{C\mu}\,,$$

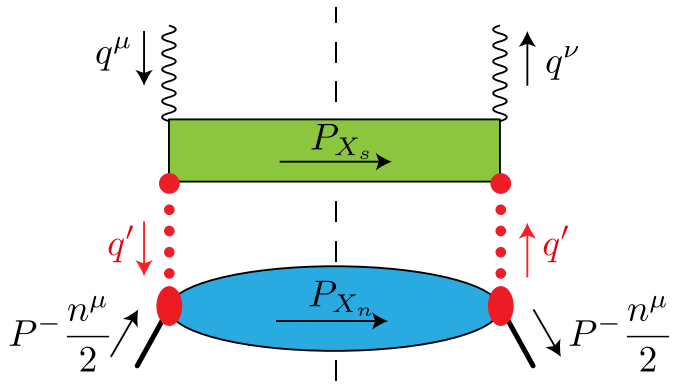

Factorization at NLL (Neill, AP, Stewart '23):

$$W^{\alpha\beta}(q,P) = \int \mathrm{d}^{d-2} q'_\perp \; S^{\alpha\beta}\left(q, q'_\perp, \frac{\nu}{x_b P^-}, \epsilon\right) \; C\left(q'_\perp, P, \frac{\nu}{P^-}, \epsilon\right) + \ldots\,.$$

Operator definitions:

$$C \equiv \frac{1}{\pi\nu}\frac{1}{q_\perp'^2} \sum_{i,j,A} \int \frac{\mathrm{d}q'^+}{2\pi} \int \mathrm{d}^d x \, e^{\mathrm{i}\frac{x^- q'^+}{2} + \mathrm{i}x_\perp \cdot q'_\perp} \langle P | \mathcal{O}_n^{i\,A}(x) \mathcal{O}_n^{j\,A}(0) | P \rangle_\nu\,,$$

$$S^{\alpha\beta} \equiv \frac{\nu}{q_\perp'^2} \frac{(2\pi\imath\mu^2)^{4-d}\left(8\pi\alpha_s(\mu^2)\right)^2}{16\pi^2\left(N_c^2-1\right)} \sum_{i,j,A} \int \frac{\mathrm{d}q'^-}{4\pi} \int \mathrm{d}^d z \, e^{\mathrm{i}z\cdot q} \int \mathrm{d}^d y_L \mathrm{d}^d y_R$$

$$\times e^{-\mathrm{i}\frac{q'^-(y_L^+ - y_R^+)}{2} - \mathrm{i}q'_\perp \cdot (y_{L\perp} - y_{R\perp})} \langle 0 | \bar{T}\{J^\alpha(z)\mathcal{O}_s^{i_n\,A}(y_L)\} T\{J^\beta(0)\mathcal{O}_s^{j_n\,A}(y_R)\} | 0 \rangle_\nu\,.$$

Small-x factorization in Glauber-SCET

A recap of small-x factorization presented last year [NPS23]

Collinear-soft interactions are mediated via the *ns*-Glauber action (Rothstein, Stewart '16) [RS16]:

$$S_G^{ns} = 8\pi\alpha_s \sum_{i,j,A} \int \mathrm{d}^d y \int \mathrm{d}^d x \int \frac{\mathrm{d}^d q'}{(2\pi)^d} \frac{e^{\mathrm{i}(x-y)\cdot q'}}{q_\perp'^2} \mathcal{O}_n^{iA}(x) \mathcal{O}_s^{j_n A}(y)\,,$$

$$\mathcal{O}_{n_i}^{qA} = \bar{\chi}_{n_i} \mathbf{T}_i^A \frac{\bar{\not{n}}_i}{2} \chi_{n_i}\,, \qquad \mathcal{O}_{n_i}^{gA} = \frac{1}{2} \mathcal{B}_{n\perp\mu}^B (\mathrm{i} f^{ABC}) \frac{\bar{n}_i}{2} \cdot (\mathcal{P} + \mathcal{P}^\dagger) \mathcal{B}_{n\perp}^{C\mu}\,,$$

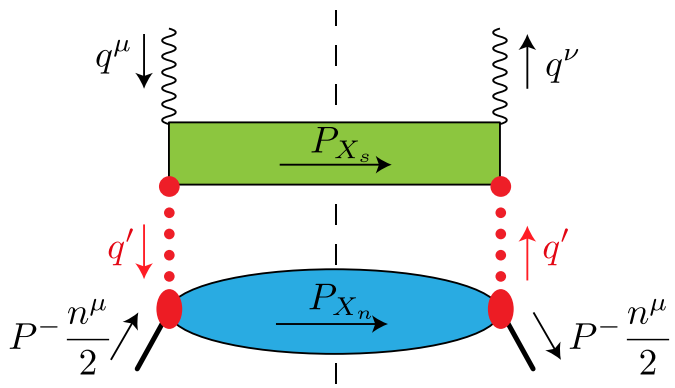

Factorization at NLL (Neill, AP, Stewart '23):

$$W^{\alpha\beta}(q,P) = \int \mathrm{d}^{d-2} q'_\perp \; S^{\alpha\beta}\left(q, q'_\perp, \frac{\nu}{x_b P^-}, \epsilon\right) \; C\left(q'_\perp, P, \frac{\nu}{P^-}, \epsilon\right) + \ldots\,.$$

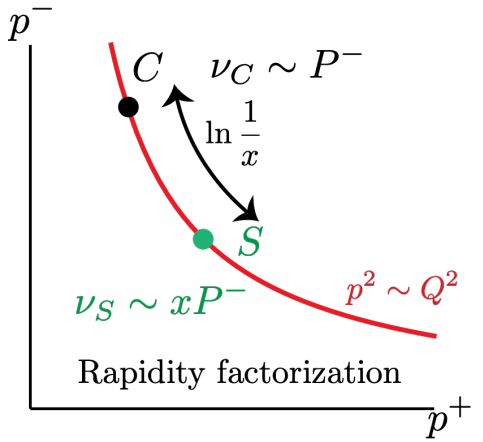

Rapidity evolution described by BFKL equation:

$$\nu \frac{d}{d\nu} C = -C - \bar{\alpha}_s \iota^\epsilon K_{\mathrm{BFKL}} \otimes_\perp C\,.$$

A straightforward extraction of twist-2 pieces (higher-power small-x pieces automatically constrained!):

$$\bar{F}^g_{L,\mathrm{HP}} + \bar{F}^g_{L,\mathrm{LL}_x}(n) = \bar{H}_L^{(g)}\left(n, \frac{Q^2}{\mu^2} = 1, \alpha_s\right) \bar{\Gamma}_{gg}(\alpha_s, n)\,,$$

$$\bar{F}^g_{2,\mathrm{HP}} + \bar{F}^g_{2,\mathrm{LL}_x}(n) = 2n_f\, \bar{\Gamma}_{qg} + \bar{H}_2^{(g)}\, \bar{\Gamma}_{gg}\,.$$

$$\frac{\nu_S}{\nu_C} = x_b$$

Why is the Glauber-SCET approach special?

Avoids many problems in the k_T-factorization framework

All existing approaches for consistent collinear and BFKL resummation are based on the k_T-factorization of Catani & Hautmann 1994 [CH94]:

$$\bar{F}_L^{(g)}(n) = h_L\left(\gamma_{gg}\right) \times R(n) \times \left(\frac{Q^2}{\mu^2}\right)^{\gamma_{gg}} \times \bar{\Gamma}_{gg} \,,$$

Why is the Glauber-SCET approach special?

Avoids many problems in the k_T-factorization framework

IR-finite, process dependent part:

$$h_L(\gamma) = \gamma \int_0^\infty \frac{\mathrm{d}\boldsymbol{k}_\perp^2}{\boldsymbol{k}_\perp^2} \left(\frac{\boldsymbol{k}_\perp^2}{Q^2}\right)^\gamma \hat{\sigma}_L^g\left(\frac{\boldsymbol{k}_\perp^2}{Q^2}, \alpha_s, \epsilon = 0\right).$$

Feature	**k_T-Factorization**	**Glauber-SCET**
Gauge Invariance	off-shell cross sections: gauge inv. only at LO	Constructed from gauge invariant Glauber ops.

Why is the Glauber-SCET approach special?

Avoids many problems in the k_T-factorization framework

$$\bar{F}_L^{(g)}(n) = h_L\left(\gamma_{gg}\right) \times R(n) \times \left(\frac{Q^2}{\mu^2}\right)^{\gamma_{gg}} \times \bar{\Gamma}_{gg} \,,$$

Feature	**k_T-Factorization**	**Glauber-SCET**
Gauge Invariance	off-shell cross sections: gauge inv. only at LO	Constructed from gauge invariant Glauber ops.
Power Counting	Obscured due to attempting simultaneous twist and high-energy factorization	Manifest power counting from the start

Why is the Glauber-SCET approach special?

Avoids many problems in the k_T-factorization framework

Define a new Green's function $\mathcal{F}_g^{(0)}$ to capture all the IR divergences:

$$\bar{F}_L^{(g)}(n) = h_L\left(\gamma_{gg}\right) \times R(n) \times \left(\frac{Q^2}{\mu^2}\right)^{\gamma_{gg}} \times \bar{\Gamma}_{gg} \,,$$

$$\bar{\mathcal{F}}_g^{(0)}\left(n, \boldsymbol{q}_\perp\right) = \frac{1}{\pi \boldsymbol{k}_\perp^2} \times \gamma_{gg} \times \tilde{R}\left(n, \boldsymbol{k}_\perp, \epsilon\right) \times \bar{\Gamma}_{gg} \,.$$

Feature	**k_T-Factorization**	**Glauber-SCET**
Gauge Invariance	off-shell cross sections: gauge inv. only at LO	Constructed from gauge invariant Glauber ops.
Power Counting	Obscured due to attempting simultaneous twist and high-energy factorization	Manifest power counting from the start
Objects	Requires auxiliary Green's functions	Nothing beyond collinear and soft functions

Why is the Glauber-SCET approach special?

Avoids many problems in the k_T-factorization framework

The BFKL $1/\epsilon_{\rm IR}$ poles are captured in the Green's function:

$$\bar{\mathcal{F}}_g^{(0)}\left(n, \boldsymbol{q}_\perp\right) = \delta^{(2-2\epsilon)}(\boldsymbol{q}_\perp) + \frac{\bar{\alpha}_s}{n}\left[K \otimes_\perp \bar{\mathcal{F}}_g^{(0)}(n)\right](\boldsymbol{q}_\perp)\,, \qquad \bar{\alpha}_s \equiv \frac{\alpha_s C_A}{\pi}$$

Feature	**k_T-Factorization**	**Glauber-SCET**
Gauge Invariance	off-shell cross sections: gauge inv. only at LO	Constructed from gauge invariant Glauber ops.
Power Counting	Obscured due to attempting simultaneous twist and high-energy factorization	Manifest power counting from the start
Objects	Requires auxiliary Green's functions	Nothing beyond collinear and soft functions
Isolating $1/\epsilon_{\rm IR}$	Additional non-trivial conversion for $1/\epsilon_{\rm IR}$ in $\overline{\rm MS}$	$S^{\alpha\beta}$ and C can be computed with $1/\epsilon_{\rm IR}$ in $\overline{\rm MS}$

Why is the Glauber-SCET approach special?

Avoids many problems in the k_T-factorization framework

IR poles in Green's function cannot be directly factorized in $\overline{\rm MS}$ scheme:

$$\bar{\mathcal{F}}_g^{(0)}\left(n, \boldsymbol{q}_\perp\right) = \frac{1}{\pi \boldsymbol{k}_\perp^2} \times \gamma_{gg} \times \tilde{R}\left(n, \boldsymbol{k}_\perp, \epsilon\right) \times \bar{\Gamma}_{gg} \, .$$

Feature	**k_T-Factorization**	**Glauber-SCET**
Gauge Invariance	off-shell cross sections: gauge inv. only at LO	Constructed from gauge invariant Glauber ops.
Power Counting	Obscured due to attempting simultaneous twist and high-energy factorization	Manifest power counting from the start
Objects	Requires auxiliary Green's functions	Nothing beyond collinear and soft functions
Isolating $1/\epsilon_{\rm IR}$	Additional non-trivial conversion for $1/\epsilon_{\rm IR}$ in $\overline{\rm MS}$	$S^{\alpha\beta}$ and C can be computed with $1/\epsilon_{\rm IR}$ in $\overline{\rm MS}$

Why is the Glauber-SCET approach special?

Avoids many problems in the k_T-factorization framework

Quark Green's function for F_2 channel:

$$G_{qg}^{(0)}\left(n, \alpha_s, \epsilon\right) = \int \mathrm{d}^{d-2}\boldsymbol{k}_\perp \, \hat{K}_{qg}\left(\frac{\boldsymbol{k}_\perp^2}{Q^2}, \alpha_s, \mu, \epsilon\right) \mathcal{F}_g^{(0)}\left(n, \boldsymbol{k}_\perp, \alpha_s, \mu, \epsilon\right).$$

Feature	**k_T-Factorization**	**Glauber-SCET**
Gauge Invariance	off-shell cross sections: gauge inv. only at LO	Constructed from gauge invariant Glauber ops.
Power Counting	Obscured due to attempting simultaneous twist and high-energy factorization	Manifest power counting from the start
Objects	Requires auxiliary Green's functions	Nothing beyond collinear and soft functions
Isolating $1/\epsilon_{\mathrm{IR}}$	Additional non-trivial conversion for $1/\epsilon_{\mathrm{IR}}$ in $\overline{\mathrm{MS}}$	$S^{\alpha\beta}$ and C can be computed with $1/\epsilon_{\mathrm{IR}}$ in $\overline{\mathrm{MS}}$
Handling collinear (non-BFKL) $1/\epsilon_{\mathrm{IR}}$	New non-BFKL $1/\epsilon_{\mathrm{IR}} \to$ new Green's functions	No mixing of BFKL and collinear $1/\epsilon_{\mathrm{IR}}$ poles.

The Collinear function

Avoids two more problems in the k_T-factorization framework

- For extension to NLL, k_T-Factorization requires computation of Impact Factors:
- Impact factors are process-dependent.
- Finite pieces are ambiguous: factorization scheme dependence.

In the EFT approach, the collinear function is universal and has a well-defined operator definition.

- NLO result for the collinear function:

$$C_q^{\rm LO}(q'_\perp) = \frac{P^-}{\nu}\frac{C_F}{\pi \boldsymbol{q}'^2_\perp},$$

$$C_q^{\rm NLO}(q'_\perp) = \bar{\alpha}_s C_q^{\rm LO} \times (-2\pi)\, I_\epsilon\left[\boldsymbol{q}'^2_\perp\right]\left(\frac{1}{\eta} + \ln\left(\frac{\nu}{P^-}\right) + \frac{3}{4}\right)$$

- Exhibits IR and rapidity poles:

$$(2\pi) I_\epsilon\left[\boldsymbol{r}_\perp^2\right] = -\frac{1}{\epsilon} + \ln\left(\frac{\boldsymbol{r}_\perp^2}{\mu^2}\right) + \mathcal{O}(\epsilon)$$

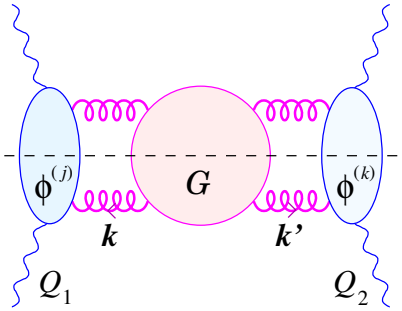

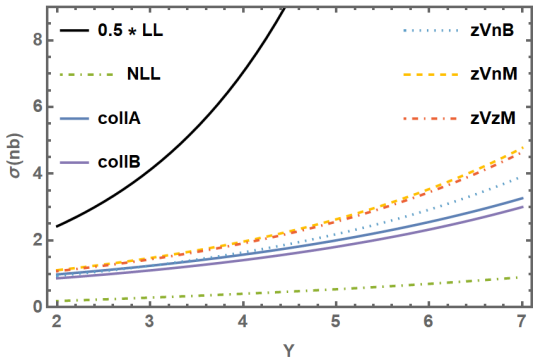

BFKL exchange contribution to $\gamma^*\gamma^*$ scattering in Colferai, Li and Stasto '23 [CLS24]

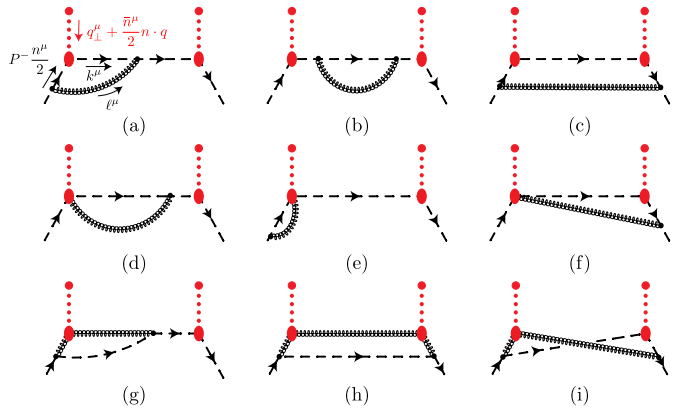

The Collinear function

Avoids two more problems in the k_T-factorization framework

- For extension to NLL, k_T-Factorization requires computation of Impact Factors:
- Impact factors are process-dependent.
- Finite pieces are ambiguous: factorization scheme dependence.

In the EFT approach, the collinear function is universal and has a well-defined operator definition.

- For NLL small x, we would like to go to two loops.
- Find over 1000 diagrams!!!

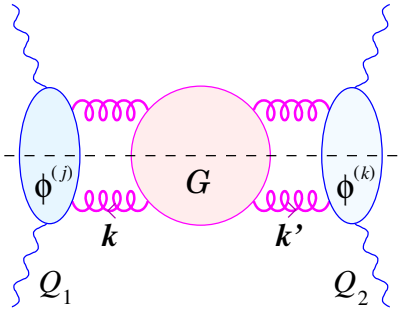

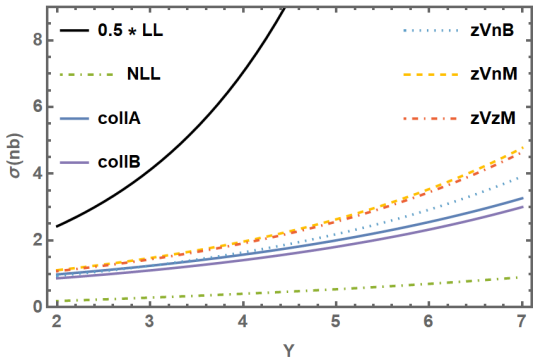

BFKL exchange contribution to $\gamma^*\gamma^*$ scattering in Colferai, Li and Stasto '23 [CLS24]

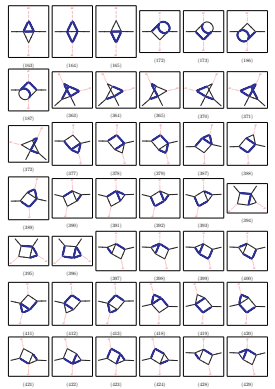

Outline

Need for automation

At two loops computing by hand becomes impractical. However, standard tools for Feynman Diagrams do not straightforwardly apply:

- SCET Lagrangian is not Lorentz Invariant
- Presence of Wilson lines leads to vertices with arbitrary valency
- Nontrivial problem to represent operators: $\chi_n, \mathcal{B}^{\mu}_{n\perp}, \mathcal{O}_n, \ldots$

The `SCETCalc` framework:

- Being built on `FeynCalc` [SMO20] development version that supports light-cone vectors.
- `QGRAF` [Nog93] to build the SCET "model"
- Automate all SCET Feynman rules
- Combine with `Tapir` [GHL23] for filtering cut diagrams
- In-house software in `Mathematica` for accessing and playing with cut edges.

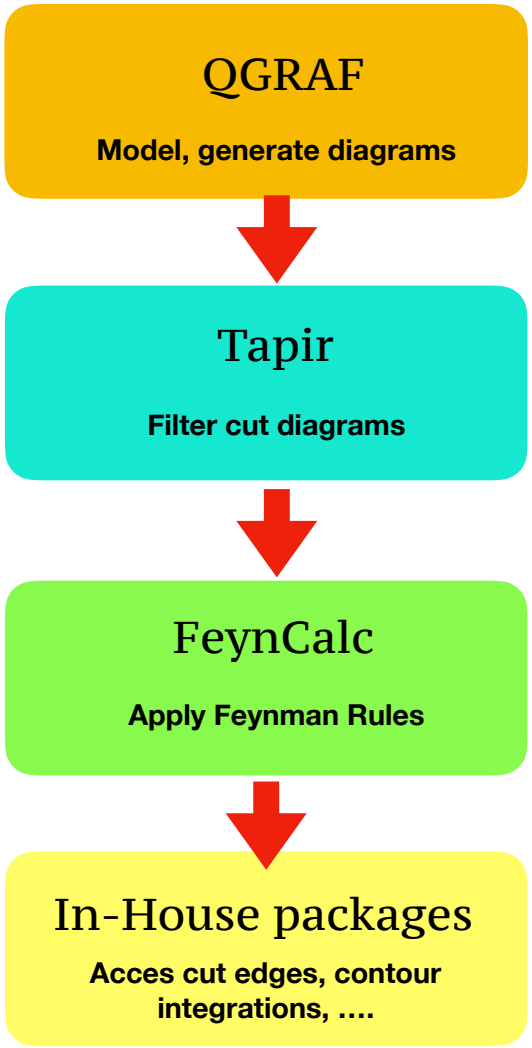

Building the Feynman rules

- Wilson lines in fundamental representation:

$$W_{n\pm}^{\dagger[N]}\left(\{k_i,\mu_i,C_i\}\right)^{a_1}{}_{a_2} = g^n \sum_{\sigma}\left(\prod_{j=1}^{N}\frac{\bar{n}^{\mu_{\sigma_j}}}{\bar{n}\cdot(q_{\sigma_1}+\ldots+q_{\sigma_j})\pm \mathrm{i}0}\right)\left(\boldsymbol{t}^{A_{\sigma_1}A_{\sigma_2}\ldots A_{\sigma_N}}\right)^{a_1}{}_{a_2}$$

- Start with operator definition (here the mid-rapidity Glauber soft operator [RS16]):

$$\chi_{n_i,\omega} = \left[\delta(\omega-\bar{n}_i\cdot\mathcal{P})W_{n_i}^{\dagger}(x)\xi_{n_i}(x)\right]$$

- Building the N-gluon Feynman rule:

$$\langle 0|\chi_{n,\omega}^{\beta}|q(s,p)g(\mu_1,k_1,C_1)\ldots\rangle = \delta\left(\omega-p^{-}-\sum_{i=1}^{N}k_n^{-}\right)W_{n_i\pm}^{\dagger[N]}\left(\{k_i,\mu_i,C_i\}\right)u_s^{\beta}(p)\,.$$

Building the Feynman rules

- Wilson lines in fundamental representation:

$$W_{n\pm}^{\dagger[N]}\left(\{k_i,\mu_i,C_i\}\right)^{a_1}{}_{a_2} = g^n \sum_{\sigma}\left(\prod_{j=1}^{N}\frac{\bar{n}^{\mu_{\sigma_j}}}{\bar{n}\cdot(q_{\sigma_1}+\ldots+q_{\sigma_j})\pm \mathrm{i}0}\right)\left(\boldsymbol{t}^{A_{\sigma_1}A_{\sigma_2}\ldots A_{\sigma_N}}\right)^{a_1}{}_{a_2}$$

- Start with operator definition (here the mid-rapidity Glauber soft operator [RS16]):

$$\mathcal{B}_{S\perp}^{\mu} = \frac{1}{n_i\cdot\mathcal{P}}\, n_i^{\nu}\, g_{\perp}^{\mu\sigma}\, S_{n_i}^{\dagger}\mathrm{i}G_{S\nu\sigma}S_{n_i}\,,$$

- Building the N-gluon Feynman rule:

$$g\mathcal{B}_{S\perp}^{\mu[N]} = \frac{n_i^{\nu}}{n_i\cdot\mathcal{P}}g_{\perp}^{\mu\rho}g^N\sum_{i=1}^{N-1}\Bigg[\sum_{\sigma(N-1)}S_n^{\dagger}\Big(\{k_{\sigma_j},\mu_{\sigma_j},C_{\sigma_j};j\in[1,i]\}\Big)G_{S\nu\rho}^{[1]}\big(\{k_{\sigma_N},\mu_{\sigma_N},C_{\sigma_N}\}\big)S_n\Big(\{k_{\sigma_j},\mu_{\sigma_j},C_{\sigma_j};j\in[i,N-1]\}\Big)$$
$$+\sum_{\sigma(N-2)}S_n^{\dagger}\Big(\{k_{\sigma_j},\mu_{\sigma_j},C_{\sigma_j};j\in[1,i]\}\Big)G_{S\nu\rho}^{[2]}\big(\{(k_{\sigma_{N-1}},\mu_{\sigma_{N-1}},C_{\sigma_{N-1}}),(k_{\sigma_N},\mu_{\sigma_N},C_{\sigma_N})\}\big)S_n\Big(\{k_{\sigma_j},\mu_{\sigma_j},C_{\sigma_j};j\in[i,N-2]\}\Big)\Bigg]\,,$$

Building the Feynman rules

- Wilson lines in adjoint representation:

$$\mathcal{S}_n^{AB[N]} = \frac{1}{T_F}\sum_{\sigma_N} \mathrm{Tr}\left[S_n^{[i]\dagger}\Big(\{k_{\sigma_j},\mu_{\sigma_j},C_{\sigma_j};j\in[1,i]\}\Big)\boldsymbol{t}^A S_n^{[N-i]}\Big(\{k_{\sigma_j},\mu_{\sigma_j},C_{\sigma_j};j\in(i,N]\}\Big)\boldsymbol{t}^B\right]$$

- Start with operator definition (here the mid-rapidity Glauber soft operator [RS16]):

$$\hat{\boldsymbol{O}}_s^{(n_i n_j)} = 8\pi\alpha_s\Big[\mathcal{P}_\perp^\mu \boldsymbol{S}_{n_i}^{\boldsymbol{g}\dagger}\boldsymbol{S}_{n_j}^{\boldsymbol{g}}\mathcal{P}_{\perp\mu} - \mathcal{P}_\perp^\mu g\boldsymbol{B}_{S\perp\mu}^{\boldsymbol{g}n_i}\boldsymbol{S}_{n_i}^{\boldsymbol{g}\dagger}\boldsymbol{S}_{n_j}^{\boldsymbol{g}} - \boldsymbol{S}_{n_i}^{\boldsymbol{g}\dagger}\boldsymbol{S}_{n_j}^{\boldsymbol{g}}g\boldsymbol{B}_{S\perp}^{\boldsymbol{g}n_j\mu}\mathcal{P}_{\perp\mu}$$
$$- g\boldsymbol{B}_{S\perp}^{\boldsymbol{g}n_i\mu}\boldsymbol{S}_{n_i}^{\boldsymbol{g}\dagger}\boldsymbol{S}_{n_j}^{\boldsymbol{g}}g\boldsymbol{B}_{S\perp\mu}^{\boldsymbol{g}n_j} - \frac{n_{i\mu}n_{j\nu}}{2}\boldsymbol{S}_{n_i}^{\boldsymbol{g}\dagger}\mathrm{i}g\boldsymbol{G}_S^{\boldsymbol{g}\mu\nu}\boldsymbol{S}_{n_j}^{\boldsymbol{g}}\Big], \qquad \mathcal{S}_{n_i}^{AB} \equiv [A|\boldsymbol{S}_{n_i}^{\boldsymbol{g}}|B]$$

- Can continue iterating:

$$\hat{\boldsymbol{O}}_s^{(n_i n_j)[1]}(-q_\perp,q'_\perp,k,\mu,C) = 8\pi\alpha_s g\Bigg[q_\perp\cdot q'_\perp\Big(\boldsymbol{S}_{n_i}^{\boldsymbol{g}\dagger[1]}(k,\mu,C)+\boldsymbol{S}_{n_j}^{\boldsymbol{g}[1]}(k,\mu,C)\Big)$$
$$-\boldsymbol{T}_g^A\left(q_{\perp\nu}\mathcal{B}_{S\perp}^{An_i\nu[1]}(k,\mu,C)+q'_{\perp\nu}\mathcal{B}_{S\perp}^{An_j\nu[1]}(k,\mu,C)+\frac{n_{i\rho}n_{j\sigma}}{2}\mathrm{i}G_S^{A\rho\sigma[1]}(k,\mu,C)\right)\Bigg]A_{S,\mu,k}^C\,.$$

Example 1: Fragmentation function

Representing operators as particles

- We represent operators such as $\chi_n, \mathcal{B}^{\mu}_{n\perp}, \ldots$ as particles and allow for multiple gluon vertices
- Include a dummy `X` to allow for propagator mixing in $\langle q|\overline{\chi}_n|0\rangle$
- Illustrate this through computation of quark fragmentation function:

$$D_{h/f}(z) = \frac{z}{2N_c}\sum_X \mathrm{Tr}\langle 0|\chi^f_n(0)|hX_n\rangle \frac{\bar{n}\!\!\!/}{2}\langle X_n h|\overline{\chi}^f_{n,p_h^-/z}(0)|0\rangle$$

- The integrand obtained using SCET Feynman rule must reproduce splitting functions:

$$J_{\kappa J} = \sum_m \sum_{\kappa^c} S_{\kappa^c} \int \mathrm{d}\Phi^c_m \sigma^c_{m,\kappa^c}\delta\big(\ldots\big)\,,$$

`QGRAF` model:

```
[ fQbar, fQ, Gl ]
[ fQbar, fQ, Gl, Gl ]
[ fQbar, fQ, Gl, Gl, Gl ]
.
.
.
[ fQbar, fChi, X ]
[ fQbar, fChi, X, Gl ]
[ fQbar, fChi, X, Gl, Gl ]
.
.
.
```

Example 1: Fragmentation function

- Interface with `Tapir` enables us to nicely isolate the desired graphs.
- Here demand single `X`, `Gl` and `fQ` passing through the cut.
- However, we would like to also access the cut edges. $\rightarrow$ re-implemented Pak's cut filter algorithm [PRS10; Hof15] as a `Mathematica` package.
- Define a relabel function:

  `{{Gl, k[1]}, {X, k[3]}, { fQ, k[2]}}`
- Enables us to always assign k_1 to the gluon:

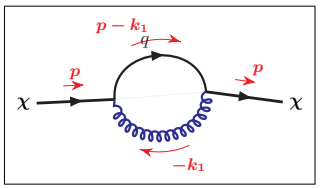

(1)

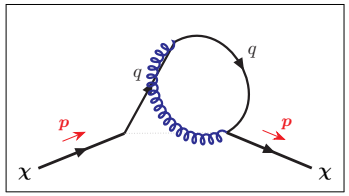

(2)

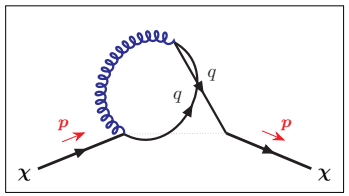

(3)

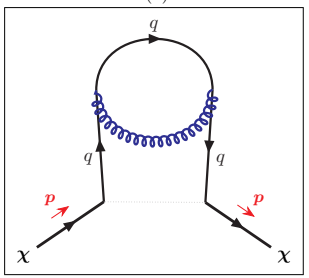

(4)

$$\texttt{Cut Edges:} \quad \begin{pmatrix} \{1,2\} & \texttt{fQ} & \{p-k_1-k_2-k_3,0\} & \texttt{C} \\ \{3,4\} & \texttt{Gl} & \{-k_1,0\} & \texttt{C} \\ \{5,6\} & \texttt{X} & \{-k_3,0\} & \texttt{M} \end{pmatrix}$$

Example 1: Fragmentation function

- Interface with `Tapir` enables us to nicely isolate the desired graphs.
- Here demand single `X`, `Gl` and `fQ` passing through the cut.
- However, we would like to also access the cut edges. $\rightarrow$ re-implemented Pak's cut filter algorithm [PRS10; Hof15] as a `Mathematica` package.
- As a cross check we verified the $P_{q_1' \bar{q}_2' q_3}$ splitting function result.

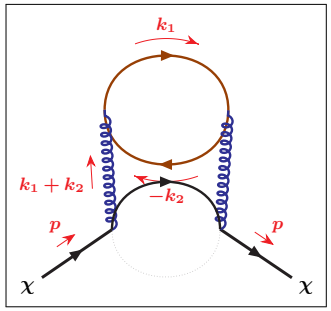

(1)

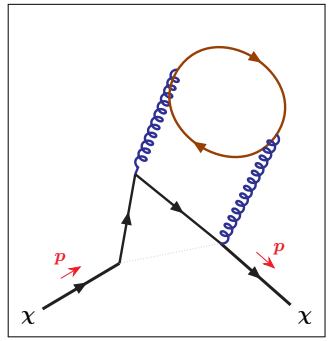

(2)

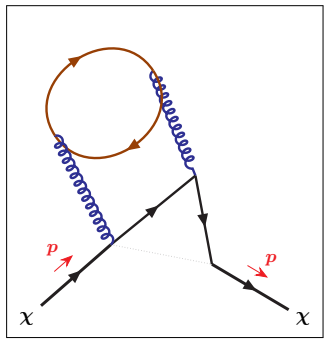

(3)

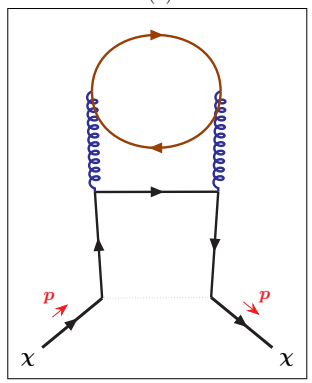

(4)

Example 2: Quark Regge trajectory

- The quark regge trajectory appears in the BFKL kernel as a virtual correction:

$$K_{\mathrm{BFKL}}(\boldsymbol{q}_\perp, \boldsymbol{k}_\perp) = \omega(\boldsymbol{q}_\perp)\delta^{(2)}(\boldsymbol{q}_\perp - \boldsymbol{k}_\perp) + K^{\mathrm{real}}_{\mathrm{BFKL}}(\boldsymbol{q}_\perp, \boldsymbol{k}_\perp)\,.$$

- Focus on the n_f pieces appearing at two-loops.

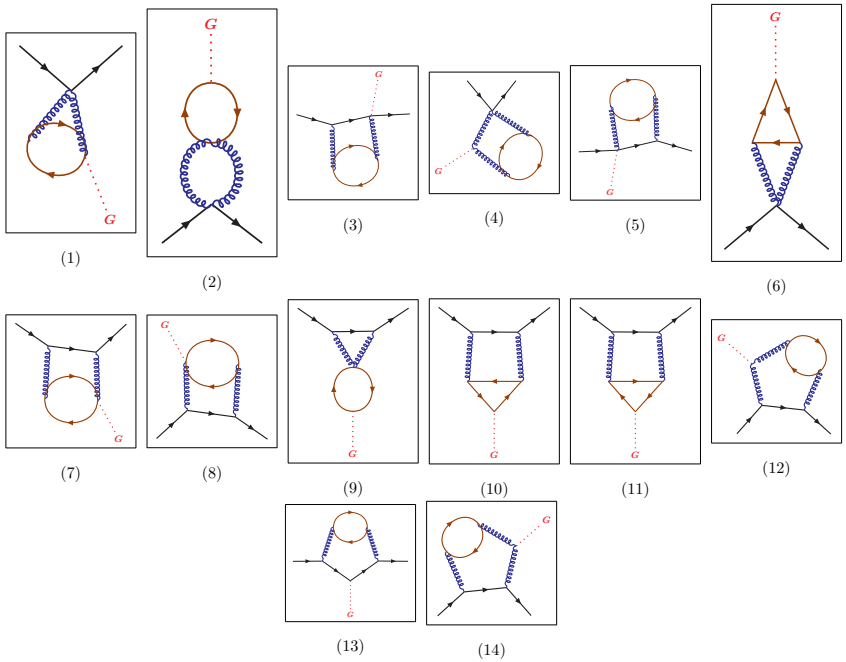

Example 2: Quark Regge trajectory

- The quark regge trajectory appears in the BFKL kernel as a virtual correction:

$$K_{\rm BFKL}(\boldsymbol{q}_\perp, \boldsymbol{k}_\perp) = \omega(\boldsymbol{q}_\perp)\delta^{(2)}(\boldsymbol{q}_\perp - \boldsymbol{k}_\perp) + K^{\rm real}_{\rm BFKL}(\boldsymbol{q}_\perp, \boldsymbol{k}_\perp)\,. \tag{10}$$

- Focus on the n_f pieces appearing at two-loops.
- Here, our in-house implementation of cut edge finder comes in very handy

  $\rightarrow$ The divergent piece arises from soft gluon limit. So always assign k_1 to the gluon, leaving the quark bubble loop to be ℓ_1.

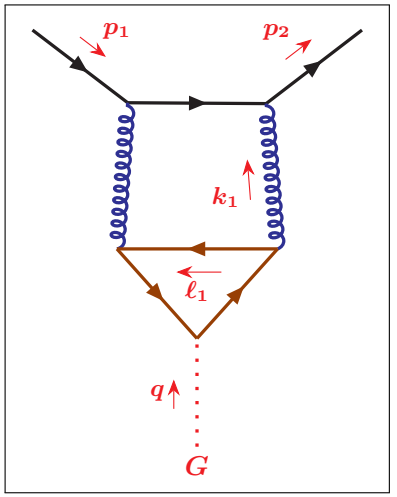

Example 2: Quark Regge trajectory

- The quark regge trajectory appears in the BFKL kernel as a virtual correction:

$$K_{\rm BFKL}(\boldsymbol{q}_\perp, \boldsymbol{k}_\perp) = \omega(\boldsymbol{q}_\perp)\delta^{(2)}(\boldsymbol{q}_\perp - \boldsymbol{k}_\perp) + K^{\rm real}_{\rm BFKL}(\boldsymbol{q}_\perp, \boldsymbol{k}_\perp)\,.$$

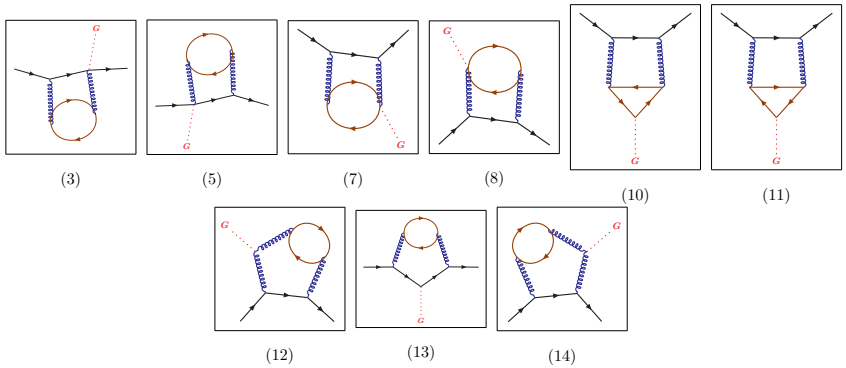

- Focus on the n_f pieces appearing at two-loops.

- Next Automate k^+ and ℓ^+ contour integration.
- For each non-zero graph we find the same constraint from the contour integral:

$$0 < |x_1| < z_1 < 1\,, \qquad x_1 \equiv \frac{\ell_1^-}{p^-} \qquad z_1 \equiv \frac{k_1^-}{p^-}$$

- Isolate all graphs that scale as $1/\lambda^2$ for $z_1 \sim x_1 \sim \lambda$.

Example 2: Quark Regge trajectory

- The quark regge trajectory appears in the BFKL kernel as a virtual correction:

$$K_{\mathrm{BFKL}}(\boldsymbol{q}_\perp, \boldsymbol{k}_\perp) = \omega(\boldsymbol{q}_\perp)\delta^{(2)}(\boldsymbol{q}_\perp - \boldsymbol{k}_\perp) + K^{\mathrm{real}}_{\mathrm{BFKL}}(\boldsymbol{q}_\perp, \boldsymbol{k}_\perp)\,.$$

- Focus on the n_f pieces appearing at two-loops.
- Additionally drop scaleless graphs: left with only two that scale as $\sim 1/\lambda^2$.
- (Final result underway)

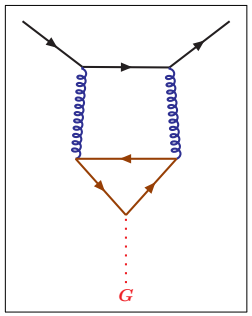

(10)

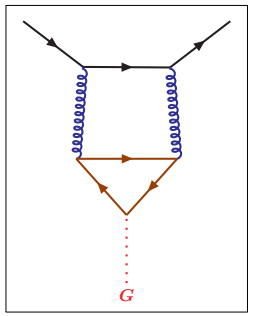

(11)

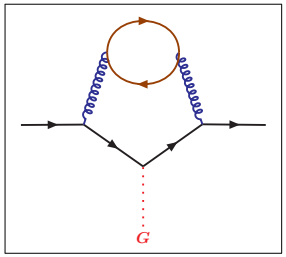

(13)

Outline

Collinear function @ NNLO: First Step

Operator definition:

$$C\left(\frac{\nu}{\bar{n}\cdot p}, q_\perp, \epsilon\right) \equiv \frac{1}{q_\perp^2}\frac{1}{\pi\nu}\sum_{i,j,A}\int\frac{\mathrm{d}n\cdot q}{2\pi}\int \mathrm{d}^d x\, e^{\mathrm{i}x\cdot q}\langle P|\mathcal{O}_n^{iA}(x)\mathcal{O}_n^{jA}(0)|P\rangle_\nu$$

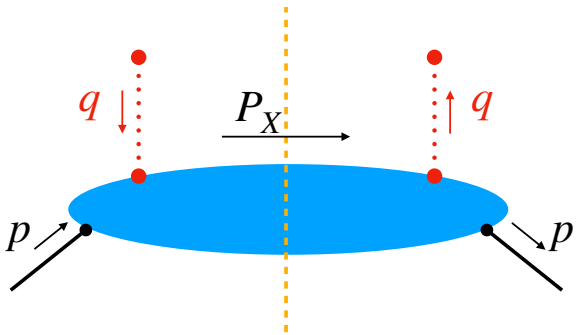

A more useful starting point for computation:

$$C_\kappa\left(\frac{\nu}{\bar{n}\cdot p}, q_\perp, \epsilon\right) = 2\int\frac{\mathrm{d}n\cdot q}{2\pi}\,\mathrm{Im}\,C_\kappa\left(\frac{\nu}{\bar{n}\cdot p}, q^\mu, \epsilon\right)$$

$$\mathcal{C}_\kappa\left(\frac{\nu}{\bar{n}\cdot p}, q^\mu, \epsilon\right) \equiv \frac{1}{q_\perp^2}\frac{1}{\pi\nu}\frac{1}{2N_\kappa}\sum_{i,j=q,g}\sum_A \mathrm{i}\int \mathrm{d}^d x\, e^{\mathrm{i}x\cdot q}\langle\kappa(P)|\mathrm{T}\left\{\mathcal{O}_n^{iA}(x)\mathcal{O}_n^{jA}(0)\right\}|\kappa(P)\rangle\,,$$

We want to make use of the Glauber collapse rule by integrating over $q^+ = n\cdot q$.

$$\begin{aligned}
&\int \mathrm{đ}q^+\mathrm{đ}\ell^+\,\frac{1}{(p+q)^2+\mathrm{i}0}\frac{1}{(\ell+p+q)^2+\mathrm{i}0}\frac{1}{\ell^2+\mathrm{i}0}\\
&= \int \mathrm{đ}q^+\mathrm{đ}\ell^+\,\frac{1}{p^-q^+ + q_\perp^2+\mathrm{i}0}\frac{1}{(\ell^-+p^-)(\ell^++q^+)+(\ell_\perp+q_\perp)^2+\mathrm{i}0}\frac{1}{\ell^-\ell^+ + \ell_\perp^2+\mathrm{i}0}\\
&= \left(\frac{-\mathrm{i}}{p^-}\right)\int \mathrm{đ}\ell^+\,\frac{\Theta(-(\ell^-+p^-))}{(\ell^-+p^-)(\ell^++q^+)+(\ell_\perp+q_\perp)^2+\mathrm{i}0}\frac{1}{\ell^-\ell^+ + \ell_\perp^2+\mathrm{i}0}\Bigg|_{q^+\to\frac{-q_\perp^2}{p^-}} = 0\,.
\end{aligned}$$

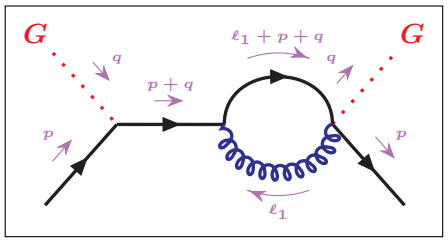

Collinear function @ NNLO: First Step

Operator definition:

$$C\left(\frac{\nu}{\bar{n}\cdot p}, q_\perp, \epsilon\right) \equiv \frac{1}{q_\perp^2}\frac{1}{\pi\nu}\sum_{i,j,A}\int\frac{\mathrm{d}n\cdot q}{2\pi}\int \mathrm{d}^d x\, e^{\mathrm{i}x\cdot q}\langle P|\mathcal{O}_n^{iA}(x)\mathcal{O}_n^{jA}(0)|P\rangle_\nu$$

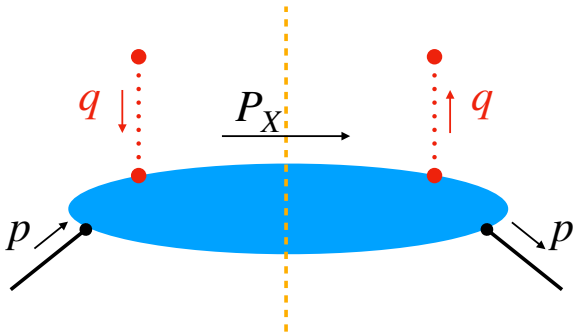

A more useful starting point for computation:

$$C_\kappa\left(\frac{\nu}{\bar{n}\cdot p}, q_\perp, \epsilon\right) = 2\int\frac{\mathrm{d}n\cdot q}{2\pi}\,\mathrm{Im}\,\mathcal{C}_\kappa\left(\frac{\nu}{\bar{n}\cdot p}, q^\mu, \epsilon\right)$$

$$\mathcal{C}_\kappa\left(\frac{\nu}{\bar{n}\cdot p}, q^\mu, \epsilon\right) \equiv \frac{1}{q_\perp^2}\frac{1}{\pi\nu}\frac{1}{2N_\kappa}\sum_{i,j=q,g}\sum_A \mathrm{i}\int \mathrm{d}^d x\, e^{\mathrm{i}x\cdot q}\langle\kappa(P)|\mathrm{T}\left\{\mathcal{O}_n^{iA}(x)\mathcal{O}_n^{jA}(0)\right\}|\kappa(P)\rangle\,,$$

We want to make use of the Glauber collapse rule by integrating over $q^+ = n\cdot q$.

- Take the imaginary part after doing $n\cdot q$ integral:

$$C_\kappa\left(\frac{\nu}{\bar{n}\cdot p}, q_\perp, \epsilon\right) = 2\,\mathrm{Im}\int\frac{\mathrm{d}n\cdot q}{2\pi}\left|\frac{n\cdot q}{\nu'}\right|^{-\eta'}\mathcal{C}_\kappa\left(\frac{\nu}{\bar{n}\cdot p}, q^\mu, \epsilon\right)$$

This requires a non-analytic regulator.

Filter graphs using collapse rule

- Exploiting the collapse rule allows us to filter a range of graphs.
- Previously these one-loop graphs were computed via taking cuts:

$$C_q^{(1),\text{real}}\left(\frac{\nu}{\bar{n}\cdot P},\vec{q}_\perp^{\,2}\right) = \frac{2\alpha_s}{\pi\vec{q}_\perp^{\,2}}\frac{\bar{n}\cdot P}{\nu} I_\epsilon\left[\vec{q}_\perp^{\,2}\right]\int_0^1 \mathrm{d}z\, P_{gq}^{\eta}(z)$$
$$\times\left[\left(C_F^2-\frac{C_F C_A}{2}\right)z^{-2\epsilon}+\frac{C_F C_A}{2}\left((1-z)^{-2\epsilon}+\boxed{1}\right)\right].$$

- All pieces except for the highlighted term cancel against virtual graphs.

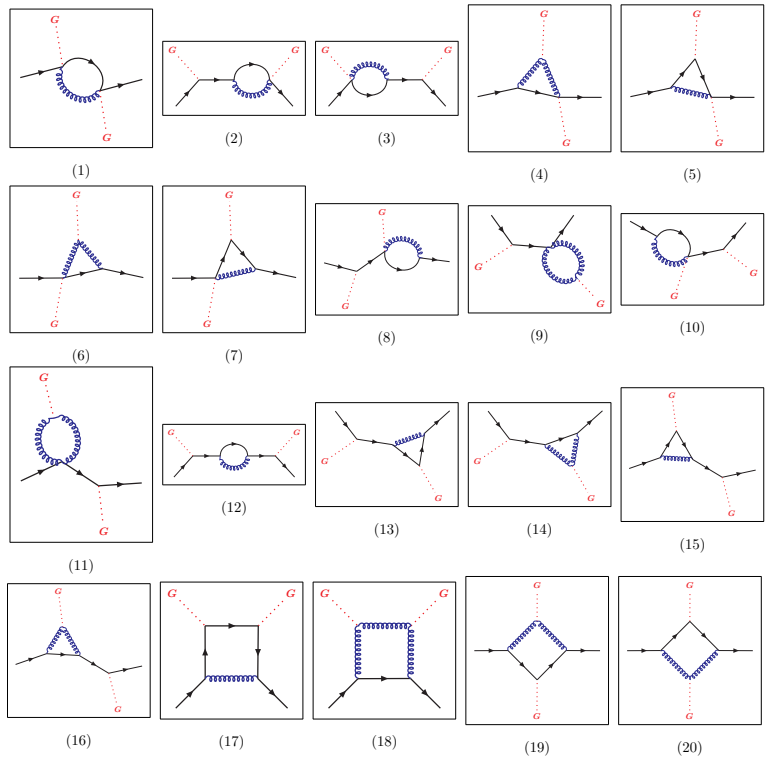

Filter graphs using collapse rule

- Exploiting the collapse rule allows us to filter a range of graphs.
- Previously these one-loop graphs were computed via taking cuts:

$$C_q^{(1),\text{real}}\left(\frac{\nu}{\bar{n}\cdot P},\vec{q}_\perp^{\,2}\right) = \frac{2\alpha_s}{\pi\vec{q}_\perp^{\,2}}\frac{\bar{n}\cdot P}{\nu} I_\epsilon\left[\vec{q}_\perp^{\,2}\right]\int_0^1 \mathrm{d}z\, P_{gq}^{\eta}(z)$$
$$\times\left[\left(C_F^2-\frac{C_F C_A}{2}\right)z^{-2\epsilon}+\frac{C_F C_A}{2}\left((1-z)^{-2\epsilon}+\boxed{1}\right)\right].$$

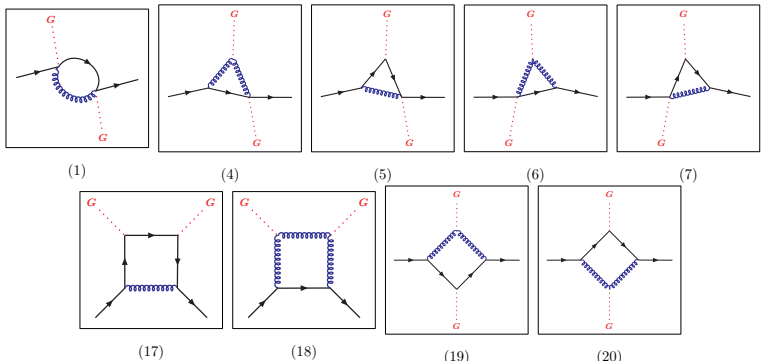

- All pieces except for the highlighted term cancel against virtual graphs.

- This can be avoided by invoking the collapse rule (implemented as ℓ_1^+ contour integration).

Filter graphs using collapse rule

- Exploiting the collapse rule allows us to filter a range of graphs.
- Previously these one-loop graphs were computed via taking cuts:

$$C_q^{(1),\text{real}}\left(\frac{\nu}{\bar{n}\cdot P},\vec{q}_\perp^{\,2}\right) = \frac{2\alpha_s}{\pi\vec{q}_\perp^{\,2}}\frac{\bar{n}\cdot P}{\nu} I_\epsilon\left[\vec{q}_\perp^{\,2}\right]\int_0^1 \mathrm{d}z\, P_{gq}^{\eta}(z) \times\left[\left(C_F^2-\frac{C_F C_A}{2}\right)z^{-2\epsilon}+\frac{C_F C_A}{2}\left((1-z)^{-2\epsilon}+\boxed{1}\right)\right].$$

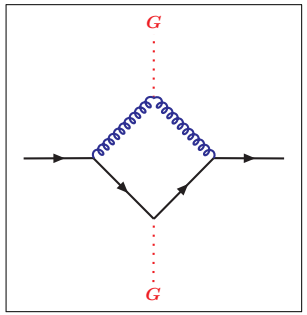

(19)

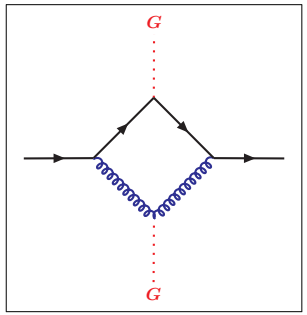

(20)

- All pieces except for the highlighted term cancel against virtual graphs.

- This can be avoided by invoking the collapse rule (implemented as ℓ_1^+ contour integration).
- Further drop scaleless integrals:
- Left with a single graph!

$$\mathcal{C}_q^{[1]} = C_F C_A g^2 \frac{P^-}{\pi\nu}\int_0^1 \mathrm{d}z \frac{1+(1-z)^2}{z}\int\frac{\mathrm{d}^{d-2}\ell_\perp}{\ell_\perp^2(\ell_\perp+q_\perp)^2},$$

NNLO graphs: What's left?

- At two loops this is a must. Start with 763 (of 1866) graphs that have valid cuts
- Applying collapse rule results in 179 graphs.

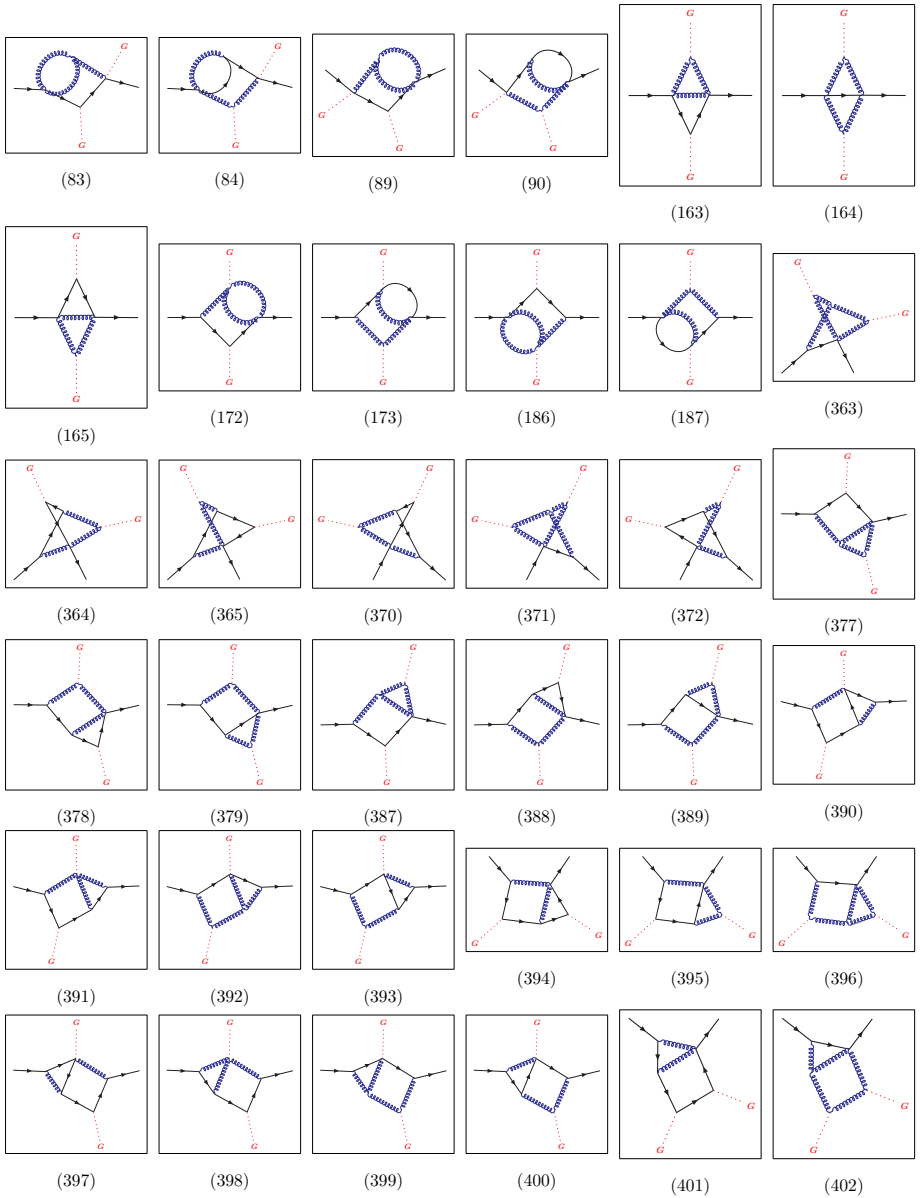

NNLO graphs: What's left?

- At two loops this is a must. Start with 763 (of 1866) graphs that have valid cuts
- Applying collapse rule results in 179 graphs.
- Further drop scaleless graphs with dangling Glaubers:

  $\rightarrow$ Left with 155 graphs.

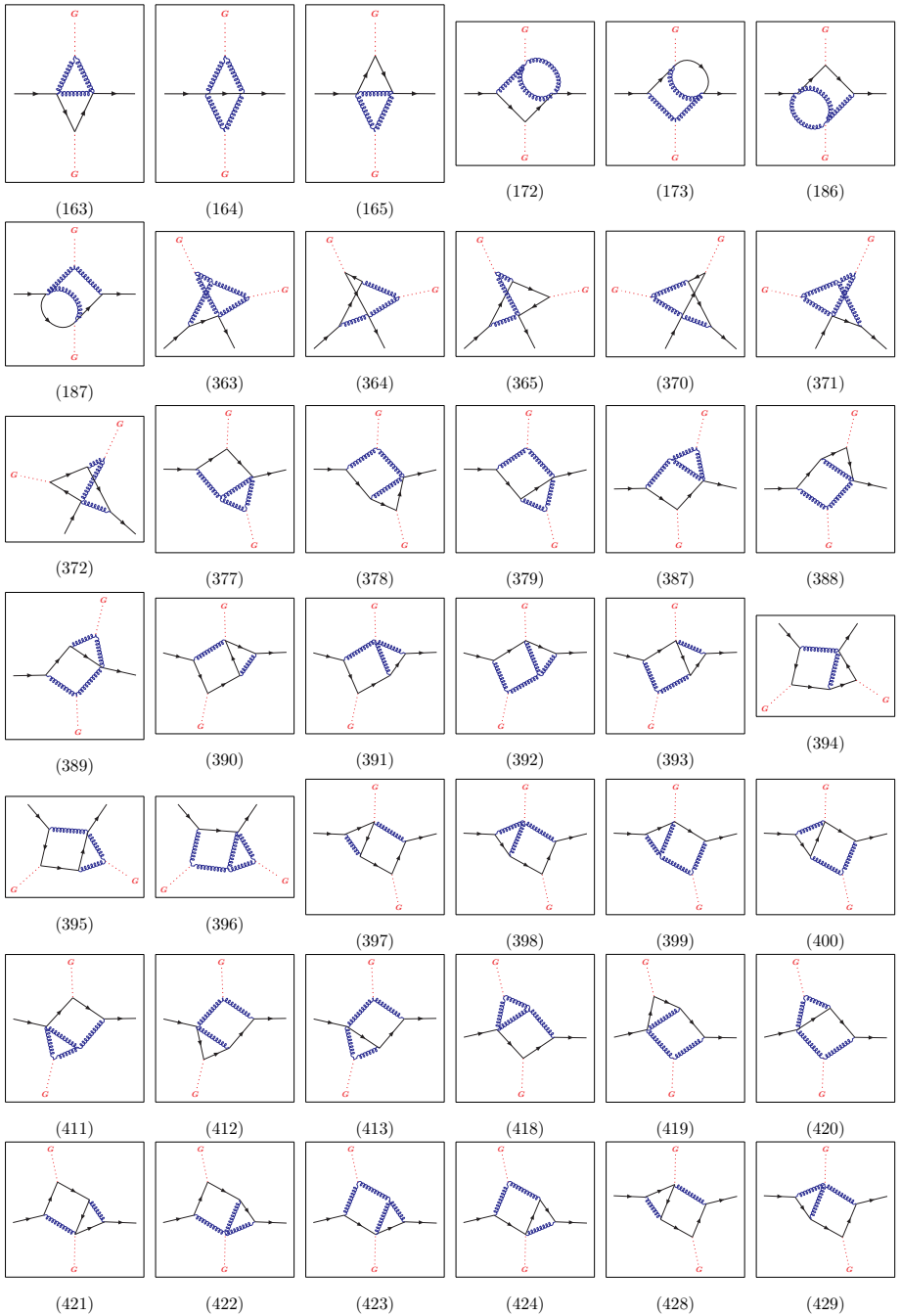

Conclusion

1. Glauber SCET is a promising framework for reliably and efficiently computing NLL small-x corrections
2. However, an extremely challenging task beyond one-loop without automation. Cannot be carried out using QCD processes.
3. Thanks to excellent packages such as `FeynCalc` and `Tapir`, this is now possible. First step in this direction.
4. While this talk focused on the specific Glauber-SCET case, the aim is to create a much more general tool-set useful for the community. Currently exploring:
   - SCET with massive quarks,
   - Subleading power operators,
   - decaying, strongly interacting resonances,
   - probe nonperturbative gluon model,
   - ...
5. Stay tuned!

Thank you!

References I

[Nog93] Paulo Nogueira. "Automatic Feynman Graph Generation". In: *J. Comput. Phys.* 105 (1993), pp. 279–289. DOI: 10.1006/jcph.1993.1074.

[CH94] S. Catani and F. Hautmann. "High-energy factorization and small x deep inelastic scattering beyond leading order". In: *Nucl. Phys.* B427 (1994), pp. 475–524. DOI: 10.1016/0550-3213(94)90636-X. arXiv: hep-ph/9405388 [hep-ph].

[FL98] Victor S. Fadin and L. N. Lipatov. "BFKL pomeron in the next-to-leading approximation". In: *Phys. Lett. B* 429 (1998), pp. 127–134. arXiv: hep-ph/9802290.

[PRS10] Alexey Pak, Mikhail Rogal, and Matthias Steinhauser. "Finite top quark mass effects in NNLO Higgs boson production at LHC". In: *JHEP* 02 (2010), p. 025. DOI: 10.1007/JHEP02(2010)025. arXiv: 0911.4662 [hep-ph].

[Hof15] Jens Simon Hoff. "Methods for multiloop calculations and Higgs boson production at the LHC". PhD thesis. KIT, Karlsruhe, 2015. DOI: 10.5445/IR/1000047447.

References II

[RS16] Ira Z. Rothstein and Iain W. Stewart. "An Effective Field Theory for Forward Scattering and Factorization Violation". In: *JHEP* 08 (2016), p. 025. DOI: 10.1007/JHEP08(2016)025. arXiv: 1601.04695 [hep-ph].

[SMO20] Vladyslav Shtabovenko, Rolf Mertig, and Frederik Orellana. "FeynCalc 9.3: New features and improvements". In: *Comput. Phys. Commun.* 256 (2020), p. 107478. DOI: 10.1016/j.cpc.2020.107478. arXiv: 2001.04407 [hep-ph].

[GHL23] Marvin Gerlach, Florian Herren, and Martin Lang. "tapir: A tool for topologies, amplitudes, partial fraction decomposition and input for reductions". In: *Comput. Phys. Commun.* 282 (2023), p. 108544. DOI: 10.1016/j.cpc.2022.108544. arXiv: 2201.05618 [hep-ph].

[McG+23] J. McGowan et al. "Approximate N^3LO parton distribution functions with theoretical uncertainties: MSHT20aN^3LO PDFs". In: *Eur. Phys. J. C* 83.3 (2023). [Erratum: Eur.Phys.J.C 83, 302 (2023)], p. 185. DOI: 10.1140/epjc/s10052-023-11236-0. arXiv: 2207.04739 [hep-ph].

[NPS23] Duff Neill, Aditya Pathak, and Iain W. Stewart. "Small-x factorization from effective field theory". In: *JHEP* 09 (2023), p. 089. DOI: 10.1007/JHEP09(2023)089. arXiv: 2303.13710 [hep-ph].

References III

[CLS24] Dimitri Colferai, Wanchen Li, and Anna M. Stasto. "Renormalization group improved photon impact factors and the high energy virtual photon scattering". In: *JHEP* 01 (2024), p. 106. DOI: 10.1007/JHEP01(2024)106. arXiv: 2311.07443 [hep-ph].